

Vascular Test Phantom Metrology For Use In Photoacoustic Applications

Liam B. Christie, William V. Giegerich, Philip J. Schneider, Kwang W. Oh

SMALL (Sensors & Micro Actuators Learning Lab) Department of Electrical Engineering
SUNY at Buffalo, Buffalo, NY, 14260, USA, liamchri@buffalo.edu

ABSTRACT

The field of photoacoustics is increasing as new discoveries are being made showing potential for a system that is capable of higher resolution medical imaging, noninvasive vital monitoring, and cancer diagnostics. This research focuses on the design, manufacturing, and testing of several test phantoms mimicking human finger vasculature for use in photoacoustic (PA) applications. Phantoms were designed for modularity, allowing the researcher to adjust channel diameter, length, depth, quantity, distention, pulse waveform, and material to meet any testing parameters. A series of different phantoms were created with these varying parameters. These phantoms were then tested with the PA system. The results of this experimentation were then compared to that of a human finger with the same test setup. A strong correlation between the output waveforms from each was observed. The change in depth with respect to the PA light source could also be observed from the captured data.

Keywords: Test phantom, human finger, photoacoustics, design, manufacturing

1 BACKGROUND & PRIOR WORK

Attempts have been made at predicting heart rate waveforms through only ultrasound [1]. PA imaging modalities present unique qualities to the medical imaging space by taking advantage of optical and acoustic imaging methods rather than pure ultrasound [2]. This allows for medical scans of physiological features to be taken at high resolution even at different depths within the human body. A current downfall of PA is a lack of quantification of system performance (such as resolution) due to the absence of devices such as test phantoms. Test phantoms are tools with known parameters used by an operator to quantify a system [3]. Previous research outlines the use of test targets created with microfluidics for quantification of PA resolution as a function of depth [4]. Further examples of both paper and acoustic test targets were found [5]. This research improves on those methods by introducing anatomically & physiologically correct test phantoms capable of showing system resolution with respect to the features found in the human body. This also allows for the controlled actuation of dynamic arteries/veins capable of pulsing at multiple different distention. Precise control of channel pressures allows for accurate duplication of the heart rate waveform.

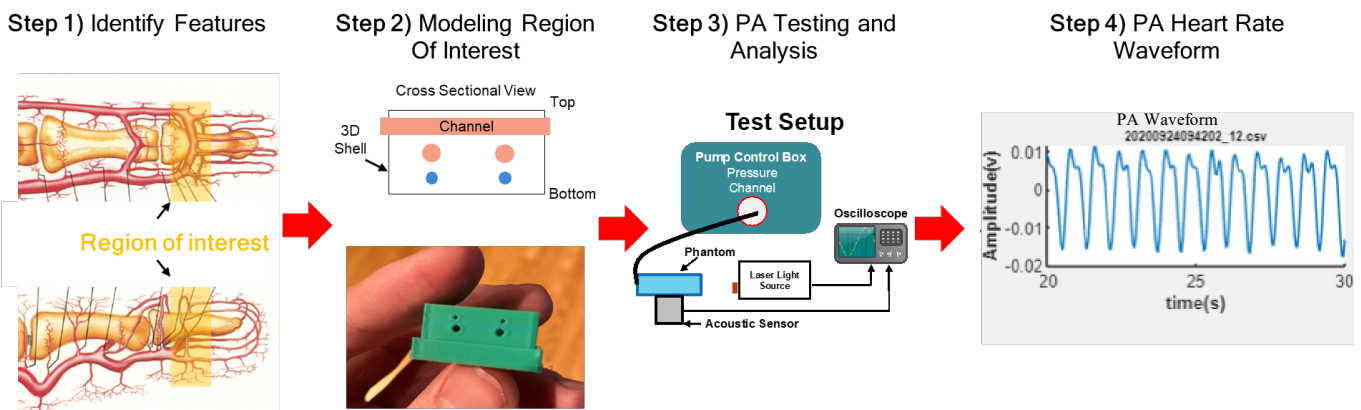


Figure 1: Representation of the process for manufacturing test phantoms. Step 1) Area of interest is identified based on test manufactured using the desired PA materials and potted in a polymer material [7]. Step 3) The phantoms are measured using a testbench consisting of the phantom, pump, laser light source, and acoustic receiver. Step 4) Data is processed through a series

2 METHODS

Test phantoms were designed to mimic the physiological characteristics of the human finger. Several material properties considered for the phantom design were extinction coefficient (combination of optical absorption and optical scattering coefficient), optical index of refraction, acoustic impedance, density, speed of sound, acoustic attenuation, Young's Modulus, and thermal expansion [8]. These parameters were tuned to closely match those of the human finger. This impacted the choice of materials for multiple different channels, phantom silicone rubbers, 3D printing PLA, and PA blood simulant (a custom manufactured mixture of black ink, water, and glycerin). A synthetic heart rate waveform was modeled after a human heart waveform captured from a photoplethysmography sensor placed on the finger. This waveform was pulsed throughout the phantom channel using a micro actuating pump capable of pulsing $\mu\text{L}/\text{min}$ with high accuracy and a PA signal was captured.

2.1 Manufacturing

A manufacturing process was developed over time to create phantoms that were repeatable and consistent across multiple different design changes and batches. Fusion 360 modeling software was used to design a 3D shell that surrounds the phantom itself. This shell served multiple main purposes. It allowed for each phantom revision to be branded with a trackable serial number which reduced confusion from batch to batch. The shell also provided support to the channels that ran throughout the phantom. An image of a 3D printed shell can be seen in Figure 2.

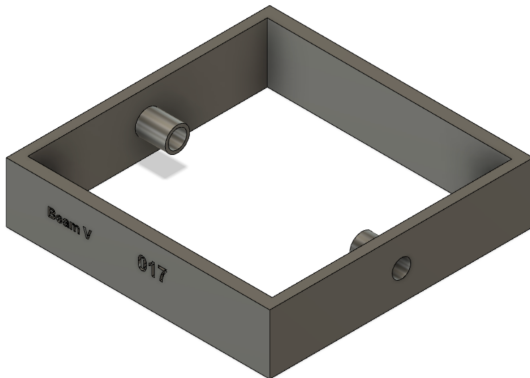


Figure 2: An image containing the 3D shell modeled within the Fusion 360 design software.

Once the shell's modeling was complete, a fused deposition modeling printer was used to create the shell. The artery/vein sizes were determined from commonly reported sizes for human artery/veins. A polymer material was used to pot the inside of the phantom shell. Once the phantoms were cured the integrity of the channels were inspected and approved underneath a laboratory inspection microscope. Finally, a realistic blood simulant was created for use in the channels of the phantom.

2.2 Heart Rate Waveform

A synthetic waveform was needed to pulse the arteries and veins within the phantom in a similar manner to that of the human body. To replicate the features of the heart rate waveform a photoplethysmography sensor was placed on the human finger and the waveform was observed and can be seen in Figure 4a. The characteristics of this waveform were then replicated and created within excel (Figure 4b).

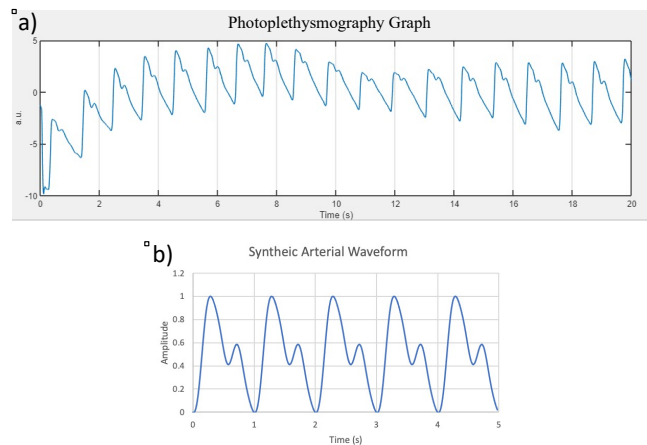


Figure 3: a) A graph of amplitude vs. time for

graph seen in a. Both of these waveforms represent arterial waveforms in the human body.

This waveform was then uploaded to a micro actuating pump in csv file format. Waveform parameters such as beat frequency/heart rate and systolic/diastolic pressure can be adjusted live time to meet any needed testing parameters of the test phantom. Phantoms can be pulsed with four unique waveforms allowing for several pressures and shapes to be used simultaneously.

2.3 Phantom Characterization

To create phantoms that closely resembled the human finger, a series of materials had to be chosen based on their properties for both acoustics and optics. All physiological features such as bone, fat, muscle, skin, and blood have known values for their optical properties. A polymer material was chosen to be the potting media for the phantom. With a broad range of distentions, phantoms could be tested through an entire spectrum of different physiological conditions such as high blood pressure, femoral artery vs. radial artery, and low blood pressure. Using a dual beam spectrophotometer, the extinction coefficient of the simulant was matched to human blood.

3 EXPERIMENTATION & RESULTS

3.1 Static Phantom Experimentation

One of the key benefits to PA is that you can determine the depth of different features within the human body using speed of sound measurements and equations. For this experimentation, three separate phantoms with channel size of 1.2mm diameter were created with varying channel depths of 8mm, 5mm, and 2mm with respect to the light source (distance measurements are to the center of the channel). Phantoms were then filled with blood simulant and

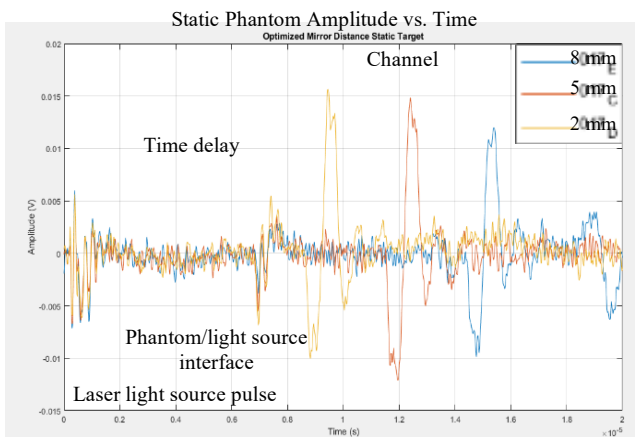


Figure 4: Raw PA signal for three separate static phantoms.

with respect to the acoustic sensor. The time delay between the laser light pulse and the arrival of the acoustic pulse at the receiver correspond to the value calculated using the speed of sound and depth of each channel.

individually placed on the light source with no pulsing waveform (static configuration). A raw PA signal was then captured for the three phantoms and the overlaid graph can be seen in Figure 5. From these raw signals the experimental channel depth can be calculated using the formula for speed of sound below where c is the speed of sound, d is the transmission distance, and t is the time of flight:

$$c = \frac{d}{t} \text{ or } d = c * t \quad (1)$$

This equation must be further manipulated to account for the distance of material leading up to the phantom that is part of the light source and the PA test bench. This must be subtracted from the distance calculation to properly receive a channel depth in polymer material. In Figure 5 the “phantom/light source interface” represents the time prior to the phantom signal. This time is roughly $7\mu s$ for the signal to reach the phantom. The equation would then be modified as shown below to account for this time for the theoretical distance calculation:

$$d = (c * (t - 7\mu s)) \quad (2)$$

The experimental channel depths were all calculated using this equation and the values can be seen in Table 1.

Actual Channel Depth (mm)	Leading Edge Channel (μs)	Calculated Channel Depth (mm)	Relative Accuracy (%)
2	8.75	1.84	92.0
5	11.5	4.73	94.6
8	14.5	7.89	98.6

Table 1: Table of actual measured channel depth, leading edge of the channel as it corresponds to Figure 5, and the calculated channel depth.

3.2 Human Finger Vs. Phantom

The main goal of this project is to create a phantom that replicates the behavior and features of the human finger and heart rate shape. In order to prove that our phantom is capable of this, an experiment was structured to include both a phantom and a live finger. A phantom was placed on the PA test system initially and a PA signal was captured. The phantom was pulsed with a 1Hz arterial waveform to achieve an adequate distention. Then a finger was placed directly on the same sensor moments later. The finger was coupled to the sensor using an ultrasonic coupling gel. A PA signal was captured for the finger with ultrasonic coupling gel. Data for

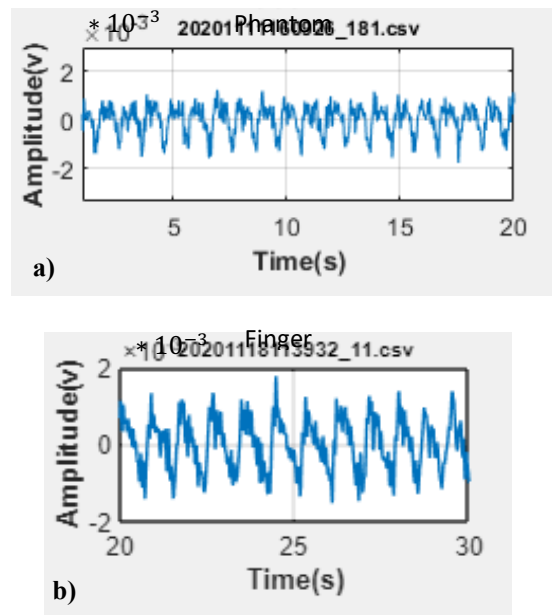


Figure 5: a) Graph of a 20 second phantom signal
finger signal when placed on the same PA setup

shape, amplitude, and frequency.

both of these experiments was exported to a csv file and graphed (Figure 6). When observing the graphs for similarities, a couple major parameters were especially important. Amplitude of the signal (signal strength) is one thing compared between the two graphs. The phantom had roughly 2mV peak to peak while the live finger had a peak to peak voltage of roughly 3mV. Frequency of the waveform was also observed throughout the experiment. The phantom is pulsing at 1 beat per second while the human finger is pulsing at 6 beats per second. This would be easily matched in the phantom by changing the frequency from 1 Hz to 1.2 Hz waveform. Finally the shape of both signals is observed. The shape in both of these graphs agrees to be a artery waveform. This is known due to the characteristic shape with the systolic (higher) peak leading the diastolic (lower) peak. With both conditions (live finger vs. phantom) maintaining the same test parameters assumptions could be made about the accuracy of the phantom as compared to the human finger. Bandpass filters could be applied to the signal to further smooth the observed graphs.

4 CONCLUSION

Test phantoms were manufactured, developed, and utilized to quantify the abilities of a PA setup. A custom 3D printed shell, polymer material, and blood simulant were fine tuned to match the human fingers acoustical and optical properties. Test phantoms provide a unique approach to testing as they remove the need for live users to prove technology with live fingers. The test phantoms themselves were built to be modular, allowing them to fit any needed testing conditions or to be altered to match a specific test subject's anatomy. Experimentation was conducted with three phantoms containing three separate channel depths. It was shown that a high accuracy can be obtained for predicting channel depth within the phantom. Experimentation was also conducted to compare a phantom and live finger. Both tests were conducted in identical testing conditions. An arterial signal could be observed from both phantom and live finger at similar amplitude, period, and relative shape.

5 FUTURE WORK

Currently phantom testing has only taken advantage of a single vessel representing an artery. Implementing two or more channels within the phantom will create an increased accuracy as compared to the human finger as multiple vessels exist within the finger. These extra channels can then be pulsed with different waveforms with varying amplitudes and beat frequencies such as a venous waveform. These channels can also be angled, curved, and uniquely implanted in order to more closely measure a vessel. Beyond that it may also be possible to mimic yet more properties of the fingers such as microstructure of the subdermal tissue. This could be a combination of multiple different polymers with separate extinction coefficients that allow for layers to be formed.

REFERENCES

- [1] Seo, J., et al. *Carotid arterial blood pressure waveform monitoring using a portable ultrasound system*. 2015 37th Annual International Conference of the IEEE Engineering in Medicine and Biology Society (EMBC). 2015.
- [2] Xu, M. and L.V. Wang, *Photoacoustic imaging in biomedicine*. Review of Scientific Instruments, 2006. **77**(4): p. 041101.
- [3] Scorza, F.O.a.S.A.S., *Use of phantoms and test objects for local dynamic range evaluation in medical ultrasounds*. 2017 IEEE International Instrumentation and Measurement Technology Conference 2017: p. pp. 1-6.
- [4] P. Schneider, N. Eadie, L. Christie, et. al., *Microfluidic Test Target for Photoacoustic Imaging*. Micro & Bio Fluidics, Lab-on-Chip, NanoTech 2018, Vol. 3 TechConnect Briefs 2018, pp. 166-169, May. 2018
- [5] Moothanchery, M. and M. Pramanik, *Performance Characterization of a Switchable Acoustic Resolution and Optical Resolution Photoacoustic Microscopy System*. Sensors, 2017. **17**(2): p. 357.
- [6] Strauch, Berish, and Wilson De Moura., *Arterial System of the Fingers*. The Journal of Hand Surgery, vol. 15, no. 1, Jan. 1990, pp. 148–154., doi:10.1016/s0363-5023(09)91123-6.
- [7] J.L. Sparks, et al. “Use of silicone materials to simulate tissue biomechanics as related to deep tissue injury.” Advances in skin and wound care 28.2(2015): 59-68.
- [8] Josef Krautkrämer, H.K., *Ultrasonic Testing of Materials*. 4th Fully Revised ed. 1983.